42 7035

N94- 33192

52-91 ABS. ONLY

p. 1

STATIONARY EDDIES IN THE MARS GENERAL CIRCULATION AS SIMULATED BY THE NASA-AMES GCM. J. R. Barnes[1], J. B. Pollack[2], and R. M. Haberle[2], [1]Oregon State University, Corvallis OR 97331, USA, [2]NASA Ames Research Center, Moffett Field CA 94035, USA.

Quasistationary eddies are prominent in a large set of simulations of the Mars general circulation performed with the NASA-Ames GCM. Various spacecraft observations have at least hinted at the existence of such eddies in the Mars atmosphere. The GCM stationary eddies appear to be forced primarily by the large Mars topography, and (to a much lesser degree) by spatial variations in the surface albedo and thermal inertia. The stationary eddy circulations exhibit largest amplitudes at high altitudes (above 30–40 km) in the winter extratropical regions. In these regions they are of planetary scale, characterized largely by zonal wavenumbers 1 and 2. Southern hemisphere winter appears to be dominated by a very strong wave 1 pattern, with both waves 1 and 2 being prominent in the northern hemisphere winter regime. This difference seems to be basically understandable in terms of differences in the topography in the two hemispheres.

The stationary eddies in the northern winter extratropics are found to increase in amplitude with dust loading. This behavior appears to be at least partly associated with changes in the structure of the zonal-mean flow that favor a greater response to wave 1 topographic forcing. There are also strong stationary eddy circulations in the tropics and in the summer hemisphere. The eddies in the summer subtropics and extratropics are substantially stronger in southern summer than in northern summer. The summer hemisphere stationary circulations are relatively shallow and are characterized by smaller zonal scales than those in the winter extratropics.

53-91 ABS. ONLY

N94- 33193

p. 2

THERMAL EMISSION MEASUREMENTS (5–25 μm) OF HAWAIIAN PALAGONITIC SOILS WITH IMPLICATIONS FOR MARS. J. F. Bell III[1] and T. L. Roush[2], [1]Mail Stop 245-3, NRC/NASA Ames Research Center, Moffett Field CA 94035-1000, USA, [2]San Francisco State University and NASA Ames Research Center, Mail Stop 245-3, Moffett Field CA 94035-1000, USA.

Background: There is ample evidence that abundant Fe-bearing minerals are present on Mars. This evidence takes the form of *in situ* analyses [1–4], previous and continuing Earth-based telescopic spectroscopic observations (reviewed in [5,6]), Viking Lander and Orbiter multispectral imaging [7–10], and Phobos 2 multispectral imaging [11,12]. Information regarding the crystalline or amorphous nature of the Fe-bearing (and other) surface materials on Mars can provide insight into the availability of liquid water at the surface and the duration, mode, and extent of weathering.

Data from Viking X-ray fluorescence analyses, magnetic experiments, and aerosol imaging were interpreted as indicating the presence of a variety of Fe-rich materials, including iron oxides [1–4,13]. However, since the Viking Landers did not carry any instruments capable of determining mineralogy, the exact mineralogical form of the Fe-bearing material remains uncertain.

Interpretations of continuing visual, near-, mid-, and far-infrared (IR) spectroscopic observations of Mars from the Earth and spacecraft over the past 20 years have revealed that the ferric mineralogy occurs in two distinct forms: (1) nanophase or truly amorphous Fe^{3+}-bearing materials [14,15] that spectrally resemble certain terrestrial palagonites [e.g., 16–20]; and (2) well-crystalline ferric oxides like hematite (α-Fe_2O_3), maghemite (γ-Fe_2O_3), or magnetite (Fe_3O_4) [1,13,15,21–24]. The available data indicate that the poorly crystalline "palagonite-like" phases are spectrally dominant [e.g., 5,6, and references within] and that the highly crystalline ferric oxides cannot constitute an abundance of more than about 4–8 wt% [24].

The research presented here represents the initial phase of a broader project that is intended to provide data in the mid- and far-IR spectral region for both well-characterized iron oxides/oxyhydroxides and poorly crystalline or amorphous materials (e.g., palagonites). Such information can be used in the interpretation of data to be returned by the Mars Observer Thermal Emission Spectrometer (TES). Additionally, this same information will prove useful for assessing the information content of existing Kuiper Airborne Observatory, Mariner 7, and Mariner 9 spectra, which also cover the thermal IR wavelength region.

Spectral Studies: In the mid IR (5–25 μm), spectral features arise from vibrational motions of atoms and molecules that compose the materials. These fundamental modes are 1–2 orders of magnitude more intense than any associated combination and/or overtones of these modes that occur at wavelengths less than 5 μm, and hence remote sensing observations in the IR are extremely sensitive to minor concentrations of these absorbing species.

From a planetary perspective, in the mid to far IR these diagnostic features occur where thermal emission rather than reflected sunlight supplies the observed photons. They occur under two sets of conditions. First, suspended particles in a nonisothermal atmosphere produce features near their vibrational fundamentals since these bands modulate the wavelength behavior of both the extinction coefficient and the single scattering albedo of the atmospheric layers within

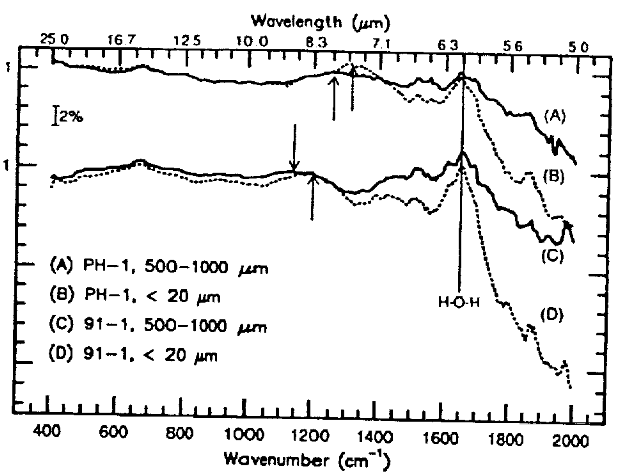

Fig. 1. Emissivity spectra of Hawaiian palagonitic samples PH-1 (thermally altered palagonitic tephra from Mauna Kea) and 91-1 (palagonitic tephra from South Point, island of Hawaii). Both coarse and fine size fraction spectra are shown. Arrows indicate subtle shifts in emissivity peak position between the two particle size regimes shown. The vertical line shows the frequency of the strong H-O-H bending fundamental caused by molecular water associated with these samples.

which they reside [25]. Second, solid and particulate surfaces exhibit spectral features in the thermal IR domain due to a spectral dependence of the surfaces' emissivity [e.g., 26,27].

Careful laboratory studies have shown that the coloring agent in certain Mars analog Hawaiian palagonitic soils is nanophase iron oxide [18,19,28]. We have measured the emissivity of two Mauna Kea palagonitic soils whose transmission spectra exhibit different spectral features [29] and of a thermally altered volcanic tephra sample that exhibits a wide range of crystallinity and degree of alteration (from black cinders to fully hematitic) [19]. Both of these samples may represent analogs for formation mechanisms involving the production of highly altered secondary weathering products on Mars. The emission spectra of all samples were measured at the TES spectroscopy laboratory [30] at Arizona State University with the cooperation of Dr. P. Christensen. The data were converted to emissivity using blackbody measurements combined with measurements of each sample at different temperatures [31].

Results: Emissivity spectra for coarse and fine particle size separates of each sample are shown in Fig. 1. Several trends are immediately obvious. First, the finer particle size fractions exhibit increasingly lower emissivity than the coarser sizes at wavenumbers above 1400 cm^{-1}. This effect may be a manifestation of the increased importance of multiple scattering at these frequencies rather than Fresnel-like reflections at lower frequencies. Second, emissivity peaks in the 1000–1400 cm^{-1} region in the fine fraction samples are shifted to higher frequencies relative to the same feature in the coarse fraction samples. This may be a particle size effect or it may be due to variations in the silicate and/or Fe-bearing mineralogy between the coarse and fine samples [e.g., 19]. While we do not make specific mineralogic assignments for the various spectral features seen in these data, we note that a broad emissivity peak possibly due to silicates is present near 1200–1300 cm^{-1} and that narrower features near 1400–1600 cm^{-1} and near 400 cm^{-1} are possibly consistent with crystalline iron oxide minerals like hematite and/or goethite [32].

This preliminary study has demonstrated that naturally occurring palagonites, thought to be good visible to near-IR spectral analogs for Mars, exhibit complex emissivity spectra at thermal wavelengths. Disentangling the various spectral signatures that make up the emissivity spectra of these complex assemblages may prove quite important in the interpretation of the Mars Observer TES data and of other mid-IR Mars datasets.

References: [1] Hargraves R. B. et al. (1977) *JGR, 82,* 4547. [2] Toulmin P. et al. (1977) *JGR, 82,* 4625. [3] Clark B. C. et al. (1977) *JGR, 82,* 4577. [4] Clark B. C. et al. (1982) *JGR, 87,* 10059. [5] Soderblom L. A. (1992) in *Mars* (H. H. Kieffer et al., eds.), 557. [6] Roush T. L. et al. (1993) in *Remote Geochemical Analysis* (C. Pieters and P. Englert, eds.), 367. [7] Soderblom L. A. et al. (1978) *Icarus, 34,* 446. [8] McCord T. B. et al. (1982) *JGR, 87,* 10129. [9] Adams J. B. et al. (1986) *JGR, 91,* 8098. [10] Arvidson R. E. et al. (1989) *JGR, 94,* 1573. [11] Murchie S. et al. (1993) *Icarus,* in press. [12] Mustard J. F. et al. (1993) *JGR, 98,* 3387. [13] Pollack J. B. et al. (1977) *JGR, 82,* 4479. [14] Morris R. V. and Lauer H. V. Jr. (1990) *JGR, 95,* 5101. [15] Morris R. V. et al. (1989) *JGR, 94,* 2760. [16] Singer R. B. et al. (1979) *JGR, 87,* 10159. [17] Evans D. L. and Adams J. B. (1980) *LPS XI,* 757. [18] Morris R. V. et al. (1990) *JGR, 95,* 14427. [19] Bell J. F. III et al. (1993) *JGR, 98,* 3373. [20] Banin A. (1992) *LPI Tech. Rept. 92-04,* 1. [21] Morris R. V. et al. (1985) *JGR, 90,* 3126. [22] Bell J. F. III et al. (1990) *JGR, 95,* 14447. [23] Hargraves R. B. et al. (1979) *JGR, 84,* 8379. [24] Bell J. F. III (1992) *Icarus, 100,* 575. [25] Toon O. B. et al. (1977) *Icarus, 30,* 663. [26] Salisbury J. W. and Eastes J. W. (1985) *Icarus, 64,* 586. [27] Salisbury J. W. et al. (1987) *JGR, 92,* 702. [28] Golden D. C. et al. (1993) *JGR, 98,* 3401. [29] Roush T. L. (1992) *LPI Tech. Rpt. 92-04,* 32. [30] Anderson D. L. et al. (1991) *LPS XXII,* 21. [31] Christensen P. R. and Harrison S. T. (1993) *JGR,* submitted. [32] Salisbury J. W. et al. (1991) *Infrared (2.1–25 μm) Spectra of Minerals,* 267, Johns Hopkins Univ.

N94-33194

54-91 ABS. ONLY

THERMAL STUDIES OF MARTIAN CHANNELS AND VALLEYS USING TERMOSKAN DATA: NEW RESULTS.

B. H. Betts[1,2] and B. C. Murray[1], [1]Mail Code 170-25, California Institute of Technology, Pasadena CA 91125, USA, [2]Now at San Juan Capistrano Research Institute, 31872 Camino Capistrano, San Juan Capistrano CA 92675, USA.

The Termoskan instrument onboard the Phobos '88 spacecraft acquired the highest-spatial-resolution thermal data ever obtained for Mars [1–3]. Included in the thermal images are 2 km/pixel midday observations of several major channel and valley systems (see Fig. 1), including significant portions of Shalbatana Vallis, Ravi Vallis, Al-Qahira Vallis, Ma'adim Vallis, the channel connecting Valles Marineris with Hydraotes Chaos, and channel material in Eos Chasma. Termoskan also observed small portions of the southern beginnings of Simud, Tiu, and Ares Valles and some channel material in Gangis Chasma. Simultaneous broad band visible data were obtained for all but Ma'adim Vallis. Here we present new results that go beyond the analysis presented in [4].

We find that most of the channels and valleys have higher inertias than their surroundings, consistent with Viking IRTM-based thermal studies of martian channels [e.g., 5–8]. We see for the first time that thermal inertia boundaries closely match all flat channel floor boundaries. Combining Termoskan thermal data, relative observations from Termoskan visible channel data, Viking absolute bolometric albedos from [9], and a thermal model of the Mars surface based upon [10], we have derived lower bounds on channel thermal inertias. Lower bounds on typical channel thermal inertias range from 8.4 to 12.5 (10^{-3} cal cm^{-2} $s^{-1/2}$ K^{-1}) (352 to 523 in SI units). Lower bounds on inertia differences with the surrounding heavily cratered plains range from 1.1 to 3.5 (46 to 147 in SI units).

Atmospheric and geometric effects are not sufficient to cause the inertia enhancements. We agree with previous researchers [5,6,8] that localized, dark, high inertia areas within channels are likely eolian in nature. However, the Termoskan data show that eolian deposits do not fill the channels, nor are they responsible for the overall thermal inertia enhancement, contrary to the IRTM-based conclusions of [6] and [8]. Thermal homogeneity and strong correlation of thermal boundaries with the channel floor boundaries lead us to favor noneolian overall explanations.

Higher inertia channel floors do not appear to be associated with catastrophic flood channels, although very few of these were observed. Eastern Ravi and southern Ares Vallis are the only two major channel segments observed that are not thermally distinct. They do not have flat floors. In contrast, channel floor inertia enhancements are strongly associated with channels showing fret-